Taylor & Francis
Taylor & Francis Group

Check for updates

RESEARCH PAPER

miR-151-5p modulates APH1a expression to participate in contextual fear memory formation

Xu-Feng Xu [a,b,c], You-Cui Wang[a], Liang Zong [d], and Xiao-Long Wang[e]

[a]Institute of Brain Science and Disease, School of Basic Medicine, Qingdao University, Qingdao, Shandong, People's Republic of China; [b]The Royal, Department of Psychiatry, and Department of Cellular and Molecular Medicine, University of Ottawa Institute of Mental Health Research, Ottawa, Canada; [c]Department of Cell and Neurobiology, School of Basic Medicine, Shandong University, Jinan, Shandong, People's Republic of China; [d]BGI-Shenzhen, Shenzhen, People's Republic of China; [e]Department of Breast Surgery, Qilu hospital, Shandong University, Jinan, Shandong, People's Republic of China

ABSTRACT

Long-term memory formation requires gene expression and new protein synthesis. MicroRNAs (miRNAs), a family of small non-coding RNAs that inhibit target gene mRNA expression, are involved in new memory formation. In this study, elevated miR-151-5p (miR-151) levels were found to be responsible for hippocampal contextual fear memory formation. Using a luciferase reporter assay, we demonstrated that miR-151 targets APH1a, a protein that has been identified as a key factor in γ-secretase activity, namely APH1a. Blocking miR-151 can upregulate APH1a protein levels and subsequently impair hippocampal fear memory formation. These results indicate that miR-151 is involved in hippocampal contextual fear memory by inhibiting APH1a protein expression. This work provides novel evidence for the role of miRNAs in memory formation and demonstrates the implication of APH1a protein in miRNA processing in the adult brain.

Introduction

The process of long-term memory formation is the progressive post-acquisition stabilization of memory. Regulation of gene expression and protein synthesis are considered to be crucial for the long-term memory formation process [1–4]. Recent studies have demonstrated given considerable attention to the epigenetic regulation of protein expression within the realm of memory formation and neuropsychiatric disorders [5,6]. Among these epigenetic mechanisms, microRNAs (miRNAs), a family of small non-coding RNAs that inhibit the expression of their target mRNAs by binding directly to their 3′- untranslated regions (UTRs), could potentially modulate the complex translational programme supporting memory [7]. miRNAs are highly expressed in the brain and their expression plays essential roles in synaptic plasticity and memory in both invertebrates and vertebrates [8–11]. miRNA-mediated regulation of gene expression has been proven to participate in spatial memory, trace conditioning, extinction memory and fear memory consolidation [12–16]. Moreover, several miRNAs have been implicated in neurodegenerative disease, such as Alzheimer's disease (AD) and Parkinson's disease (PD) [17–22]. In addition to the characterized miRNAs, many other miRNAs are enriched in the brain, but their functions in learning and memory are still largely unknown.

In this paper, we used an unbiased microarray-based miRNome-wide screening to study the miRNAs involved in hippocampal contextual fear memory. Our work revealed that miR-151-5p (miR-151), a miRNA that co-expresses with focal adhesion kinase (FAK) and has been reported to be involved in both cancer and cardiac hypertrophy [23–29], was involved in hippocampal long-term memory formation. Using a luciferase reporter assay, we identified a target of miR-151, APH1a, which is a component of the gamma secretase complex that cleaves integral membrane proteins such as Notch receptors and beta-amyloid precursor proteinmiR-151. Finally, we demonstrated that miR-151 upregulation could reduce target APH1a protein levels and thus facilitate the formation of hippocampal fear memory.

Results:

miR-151 is upregulated in the hippocampus 1 h after contextual fear conditioning

To evaluate the miRNAs associated with CFC memory, a microarray was performed on miRNA extracted from the hippocampus of adult mice 1 h after contextual fear conditioning (CFC) training (Figure 1(a, b)). Hundreds of miRNAs were read by the microarray. miRNAs with a signal greater than 500 were chosen for further analyses. The results indicated a dynamic regulation of 38 miRNAs (p < 0.05) during the period in which fear memory consolidation occurs (Table 1). To verify whether these miRNAs were indeed changed in a learning-dependent manner, we used qPCR to quantify the levels of these miRNAs 0 h, 1 h and 6 h after CFC training (Figure 1(c)). Training data showed that the
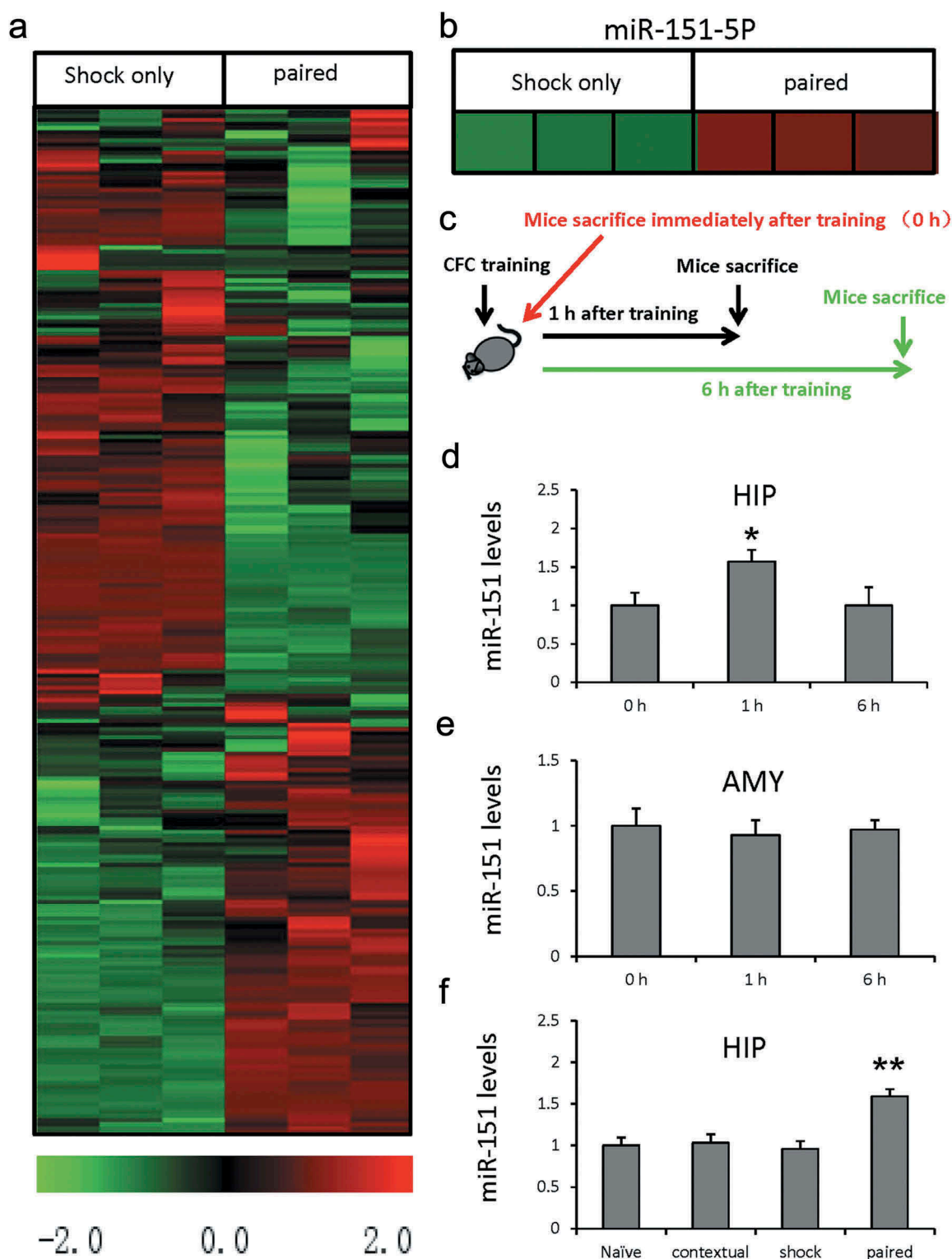
Figure 1. miRNA expression profiling and qPCR confirmation showed miR-151 is increased in the hippocampus 1 h after contextual fear conditioning.

(a,b) miRNA levels in the hippocampus of fear-conditioned adult male mice compared to shock-only controls were profiled using an array-based approach (Green-Black-Red: low to high miRNA levels). (c) The schematic diagram for describing our experimental design. D. qPCR analysis showed the relative levels of miR-151 in the hippocampus of mice 1 h and 6 h after CFC training (n = 4 per group; *p < 0.05 vs 0 h group). E. Temporal changes of miR-151 levels in the amygdala following CFC training using qPCR (n = 5–6 per group). F. Relative levels of miR-151 in the hippocampus 1 h after context alone, immediately shock alone, or paired CFC training normalized to control (n = 5 per group; **p < 0.01 vs naive group). All values are presented as the mean ± SEM.

mice spent more time freezing as the number of electric shocks increased, indicating that they have successfully completed the learning process (Supplementary Figure 1). Our results revealed that the levels of miR-151 increased significantly 1 h after training in the hippocampus (Figure 1(d), $F_{(2,9)} = 3.961$, $p = 0.028$, one-way ANOVA), which suggested that miR-151 could be involved in

Table 1. the hippocampal miRNAs changed at 1 h after CFC training (Signal>500, $p < 0.05$).

Reporter Name	Group 1 (Shock only)		Group 2 (Paired)		Log2 (G2/G1)
	Mean	StDev	Mean	StDev	
mmu-miR-1196-5p	47	2	1,199	57	4.68
mmu-miR-690	2,364	33	1,111	28	−1.09
mmu-miR-133b-5p	5,166	315	221	24	−4.55
mmu-let-7d-5p	1,795	19	1,146	17	−0.65
mmu-miR-181a-5p	2,433	37	3,635	42	0.58
mmu-miR-151-5p	876	18	1,393	28	0.67
mmu-miR-342-3p	1,446	55	732	19	−0.98
mmu-miR-143-3p	548	11	843	34	0.62
mmu-miR-103-3p	906	36	1,352	34	0.58
mmu-miR-341-5p	42,039	653	36,765	335	−0.19
mmu-miR-150-5p	611	31	337	23	−0.86
mmu-miR-30d-5p	1,294	61	735	50	−0.81
mmu-miR-107-3p	874	21	1,264	14	0.53
mmu-miR-6239	11,682	300	15,310	562	0.39
mmu-let-7f-5p	1,840	24	1,289	34	−0.51
mmu-miR-126-3p	503	23	861	76	0.78
mmu-miR-487b-3p	582	41	1,003	73	0.78
mmu-miR-24-3p	1,435	62	1,032	52	−0.48
mmu-let-7a-5p	2,494	19	1,494	91	−0.74
mmu-miR-195a-5p	964	37	1,246	73	0.37
mmu-miR-29a-3p	933	17	1,228	47	0.40
mmu-miR-127-3p	1,287	38	2,049	155	0.67
mmu-miR-128-3p	5,704	110	7,084	295	0.31
mmu-miR-222-3p	632	22	1,096	127	0.79
mmu-miR-26a-5p	6,230	211	8,584	573	0.46
mmu-miR-30b-5p	2,104	137	2,696	179	0.36
mmu-miR-125a-5p	3,117	154	2,403	213	−0.38
mmu-miR-23a-3p	1,435	40	1,039	86	−0.47
mmu-let-7b-5p	1,025	32	691	73	−0.57
mmu-miR-99b-5p	1,130	59	1,368	82	0.28
mmu-miR-16-5p	2,207	55	2,384	48	0.11
mmu-miR-99a-5p	1,751	20	1,546	51	−0.18
mmu-miR-139-5p	787	54	956	40	0.28
mmu-miR-100-5p	1,174	51	1,008	49	−0.22
mmu-miR-125b-5p	6,268	227	4,630	454	−0.44
mmu-miR-30c-5p	4,271	128	4,686	153	0.13
mmu-miR-124-3p	10,808	391	12,097	527	0.16
mmu-miR-140-3p	603	40	967	151	0.68

hippocampal fear memory. Interestingly, the levels of miR-151 in the amygdala, another brain region involved in CFC memory formation, did not change significantly after CFC training (Figure 1(e)). We then investigated whether the CFC training-induced miR-151 increase was specific to associative fear learning rather than exposure to either context or shock alone. Our results revealed that neither context alone nor shock alone could upregulate miR-151 (Figure 1(f), $F_{(3,16)} = 9.880$, $p = 0.001$, one-way ANOVA), suggesting that increased miR-151 was specific to the associated hippocampal memory.

Manipulation of miR-151 in the hippocampus affects the consolidation of contextual fear conditioning

To examine whether the increased miR-151 was functionally involved in hippocampus-dependent memory, we stereotactically injected antagomirs against miR-151 (miR-151-anta) into the DG of adult mice to reduce the levels of miR-151. qPCR results showed that miR-151 levels in DG were decreased to 27.8% after injection of antagomirs (Figure 2(b), $p < 0.001$, two-tailed t test). These results suggest that the antagomirs effectively blocked the levels of miR-151 in adult mice. Next, a miR-151 overexpression lentivirus, which simultaneously expressed GFP protein, was injected into mouse DG. One month later, numerous GFP-positive cells in were detected in the DG of lentivirus-injected mice (Figure 2(a)), which suggested that the DG was successfully transfected by the lentivirus. qPCR results showed that miR-151 levels in the DG increased by 85.5% after lentivirus injection when compared to control values (Figure 2 (b), $p < 0.001$, two-tailed t test). These results suggested that lentiviral miR-151 overexpression effectively increased miR-151 levels in the hippocampus.

Next, we evaluated the effect of miR-151 knockdown on hippocampal-dependent memory. We subjected two groups
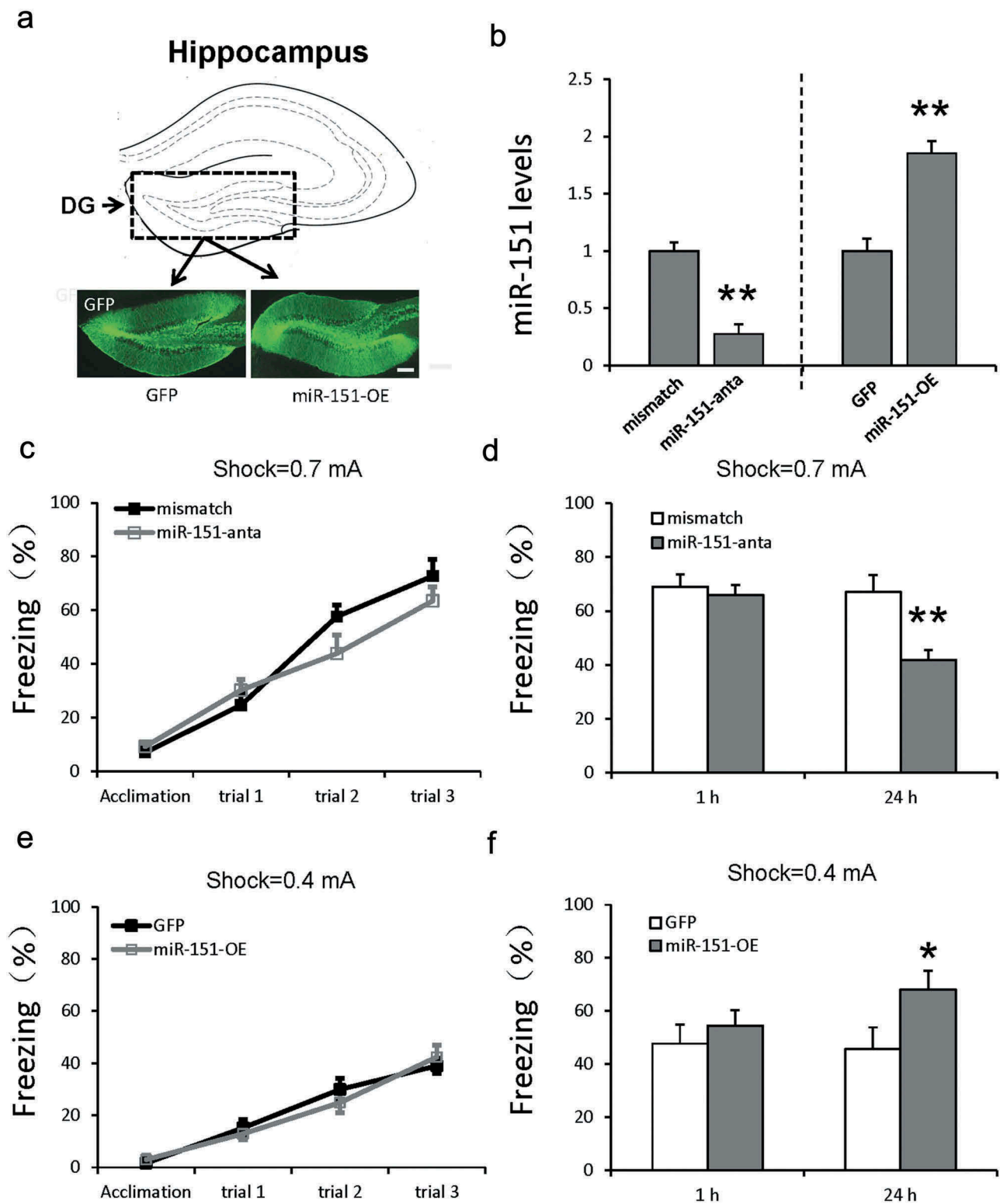
Figure 2. Manipulation of miR-151 in the hippocampus affects CFC memory formation.

(a) The location and diffusion range of miR-151-overexpression lentivirus microinjected into DG (scale bar, 200 μ m). B. Relative levels of miR-151 in the DG after miR-151 antagomir or overexpression lentivirus injection (n = 5–7 per group; **p < 0.01 vs Mismatch group; **p < 0.01 vs GFP group). (c, d) miR-151 knockdown impaired contextual fear memory. (c) The freezing response during the training process. (d) The freezing response 1 h and 24 h after training (n = 10–11 per group; **p < 0.01 vs 24 h Mismatch group). (e, f) miR-151 overexpression enhanced contextual fear memory following a weak electric shock. (e). The freezing response in training. (f). The freezing response 1 h and 24 h after training (n = 7–10 per group; *p < 0.05 vs 24 h GFP group). All values are presented as the mean ± SEM.

of mice (mismatch and miR-151-anta) to the contextual fear conditioning test. Both groups of mice exhibited an intact freezing response during the training process (Figure 2(c)),

which suggested that abolishing miR-151 had no effect on contextual fear memory acquisition. We then examined short-term memory (STM) 1 h after training and long-term

memory (LTM) 24 h after training. Freezing time was not significantly different between the two groups in the STM test (Figure 2(d)). However, in the LTM test, mice injected with antagomirs showed a significant decrease in freezing time compared with mice in the mismatch group (Figure 2(d)), $p = 0.0027$, two-tailed t test), which suggested that blocking miR-151 could impair long-term memory formation.

We then used lentiviral miR-151 overexpression to examine whether overexpressing miR-151 could affect long-term memory formation. To avoid a ceiling effect, we used a weak electric shock to condition the mice. Our results showed that mice in both groups exhibited similar freezing times during CFC training (Figure 2(g)) and the STM test (Figure 2(h)), which suggested that miR-151 overexpression had no effect on contextual fear memory acquisition and STM. However, in the LTM test, mice injected with the miR-151 overexpression lentivirus exhibited significantly increased freezing time compared with GFP control mice (Figure 2(h), $p = 0.025$, two-tailed t test); this suggested that miR-151 overexpression could enhance the formation of contextual fear memory. Taken together, these results suggest that miR-151 is involved in the formation of contextual fear memory.

Decreasing miR-151 could not affect anxiety-like behaviour

The above data revealed that miR-151 could participate in CFC consolidation. To examine whether miR-151 could participate in other emotion or memory systems, we observed auditory cued for fear memory after injection with miR-151 antagomirs in dorsal hippocampus. We found no difference in freezing behaviours between scramble and injected antagomirs groups (Figure 3(a, b)), suggesting that miR-151 inhibition in the dorsal hippocampus does not affect the cued fear memory. We then subjected mice to the Morris water maze test, another hippocampus-dependent memory behavioural test, and we found that in comparison to control mice, the mice in which miR-151 was inhibited had significantly increased escape latency in the hidden platform trials (Figure 3(c), group, $F_{(1,56)} = 5.011$, $p = 0.046$; training trial, $F_{(4,56)} = 37.815$, $p < 0.001$; interaction, $F_{(4,56)} = 1.820$, $p = 0.149$, repeated measured two-way ANOVA), decreased numbers of platform crossings (Figure 3(d), $p = 0.0031$, two-tailed t test) and spent less time in the target quadrant during the probe test (Figure 3(e), $p < 0.001$ two-tailed t test), suggesting that blocking miR-151 impairs spatial memory. To examine whether miR-151 participates in emotion, we used the open field and elevated plus maze tasks. Our results demonstrated that locomotion and time spent in the centre of the open field were similar in antagomir-injected mice and mismatch mice. This finding suggests that blocking miR-151 does not affect spontaneous exploratory activity and anxiety-like behaviour. In the elevated plus maze, miR-151 knockdown showed that time spent in the open arm and frequency into the open arm were the same. These results suggested that blocking miR-151 did not affect anxiety-like behaviour (Figure 3(f-i)).

APH1a is the target of miR-151

The above results showed that miR-151 was essential for CFC memory formation, but the underlying mechanism was still unknown. Next, we wanted to uncover the targets of miR-151 that participate in hippocampal memory. In scanning the 3′ UTRs of mRNAs for potential miR-151 binding sites, we identified APH1a, a component of the gamma secretase complex that cleaves integral membrane proteins such as Notch receptors and beta-amyloid precursor protein. We then used a luciferase reporter assay to ask whether APH1a was indeed a molecular target of miR-151. The 3′ UTR of APH1a was cloned downstream of luciferase. When HEK293 cells were cotransfected with a construct encoding miR-151 and the luciferase construct with the 3′ UTR of APH1a, luciferase-mediated luminescence was significantly decreased compared to control values (Figure 4(a), $F_{(4,15)} = 10.688$, $p < 0.001$, one-way ANOVA). However, luminescence was intact when the seed region of APH1a was mutated (Figure 4(a)). These results suggest that the 3′ UTR of APH1a was targeted by miR-151 to suppress luciferase activity. When we blocked the function of miR-151 using antagomirs, the luminescence was rescued (Figure 4(a), $p < 0.001$, one-way ANOVA). Moreover, we blocked or overexpressed miR-151 in human HEK293 cells and found that blocking miR-151 significantly increased APH1a protein levels (Figure 4(b,c), $F_{(2,9)} = 31.056$, $p = 0.0045$, one-way ANOVA), while overexpressing miR-151 significantly decreased APH1a protein levels in HEK293 cells (Figure 4(b,c), $p = 0.0026$, one-way ANOVA). These results suggested that APH1a was the target of miR-151.

miR-151 induces a decrease in APH1a protein levels after CFC training

The above results showed that the expression APH1a is a target of miR-151; next, we investigated whether this target was regulated by miR-151 after CFC training. First, we examined APH1a protein levels after CFC training and found that the protein level was decreased 4 h after CFC training (Figure 5(a,b), $F_{(5,26)} = 23.233$, $p < 0.001$, one-way ANOVA).

Since we found the levels of APH1a were decreased after CFC training, next we wanted to investigate whether these changes were regulated by miR-151 in mice. We used antagomirs to block miR-151 and then subjected mice to CFC training. Mice were randomly divided into 4 groups: homecage+vehicle (HC+veh), homecage+miR-151-antagomirs (HC+151-anta), CFC+vehicle (CFC+veh), CFC+miR-151-antagomirs (CFC+151-anta). Compared with HC+veh group, APH1a levels were increased in mice of HC+151-anta group which suggested that blocking miR-151 can elevate the levels of APH1a (Figure 5(c,d), antagomir, $F_{(1,15)} = 116.344$, $p < 0.001$, two-way ANOVA). We observed that mice in the CFC+veh group showed decreased APH1a protein levels compared with HC+veh group mice 4 h after CFC training (Figure 5(d), CFC, $F_{(1,15)} = 5.305$, $p = 0.039$, two-way ANOVA). However, when given antagomirs, mice in the CFC+151-anta group showed significantly increased APH1a protein levels compared with mice in CFC+veh group (Figure 5(d), antagomir × CFC interaction, $F_{(1,15)} = 8.387$, $p = 0.013$, two-way ANOVA), which suggested that the reduced APH1a protein levels that follow CFC training are regulated by miR-151 in mice.
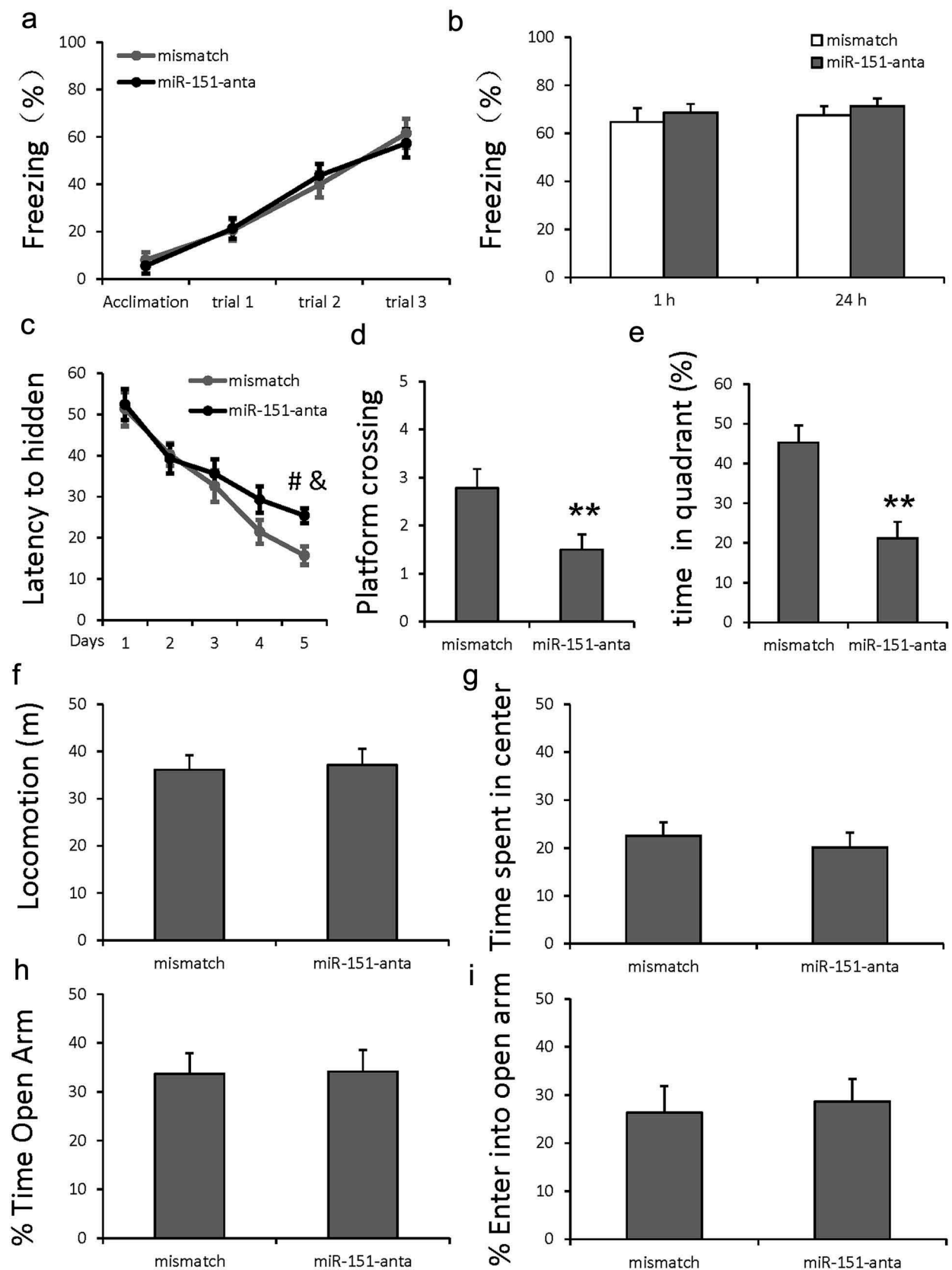
Figure 3. Decreasing miR-151 impaired spatial memory but not cued fear memory or anxiety-like behaviour.

(a, b) miR-151 knockdown has no effect on cued fear memory process. (a) The freezing response during training. (b) The freezing response 1 h and 24 h after training (n = 8–9 per group). (c-f) miR-151 knockdown impaired the spatial memory in the Morris water maze test. (c) The escape latency to find the hidden platform over four consecutive days (n = 8 per group, #: significant group effect; &: significant training trial effect). (d) The number of platform crossings in the target quadrant during the probe test (n = 8 per group, **p < 0.01 vs Mismatch group). (e) The time spent in the target quadrant during the probe test (n = 8 per group, **p < 0.01 vs Mismatch group). F.G. Mice injected with miR-151-antagomir exhibited the same locomotion and time spent in centre compared with mismatch group in the open field test (n = 8 per group, two-tailed T test). H, I. Mice injected with miR-151-antagomir showed similar time spent in the open arms and frequency into the open arms compared with mismatch group in the elevated plus maze test (n = 8 per group, two-tailed T test). All values are presented as the mean ± SEM.

a

miR-151 3'TGATCTGACACTCGAGGAGCT5'
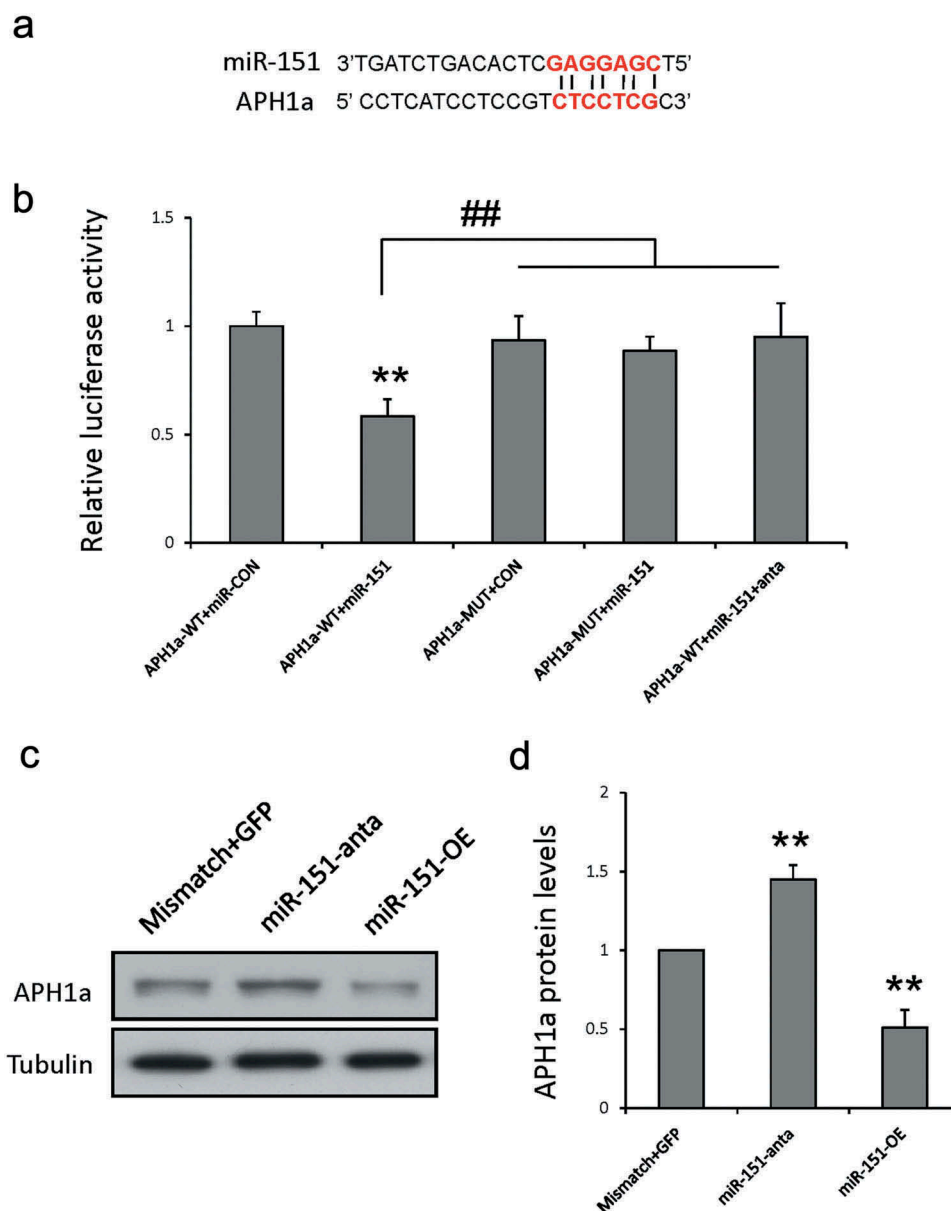APH1a 5' CCTCATCCTCCGTCTCCTCGC3'

b

c

d

Figure 4. APH1a is a target of miR-151.
(a) Sequence analysis shows that the sites of APH1a completely matched with the seed sequence of miR-151. B. The luciferase assay was used to demonstrate that APH1a is a target of miR-151 (n = 4 per group; **p < 0.01 vs APH1a-WT+miR-CON group). (c, d) Knockdown or overexpression APH1a affected APH1a protein expression in HEK293 cells (n = 4 per group; **p < 0.01 vs Mismatch+GFP group). Representative immunoblots are shown in C, and the relative densitometric analysis is shown in D. All values are presented as the mean ± SEM.

Taken together, these results suggested that miR-151 could reduce the protein levels of its target, APH1a, following CFC training.

APH1a in the hippocampus is involved in fear memory consolidation

Our above data revealed that miR-151 could decrease APH1a protein levels after CFC training; however, it was still unclear whether the effect of miR-151 on the formation of fear memory is dependent on APH1a. To this end, we first examined whether APH1a was functionally involved in hippocampus-dependent memory. For this purpose, we used a si-APH1a lentiviral vector, which coexpressed GFP, to knock down APH1a levels in DG and an APH1a-overexpression lentiviral vector that encoded APH1a-GFP, a fusion protein of APH1a and GFP, to overexpress the APH1a protein. We then subjected mice to CFC training and testing to examine the function of APH1a in hippocampus-dependent memory. Mice exhibited similar freezing responses regardless of whether APH1a was knocked down or overexpressed APH1a in DG when given CFC training and during the test 1 h after training (Figure 6(a, c)), which suggested that APH1a was not involved in contextual fear memory acquisition and STM process. However, when tested 24 h after training, mice injected with the APH1a-overexpression lentivirus exhibited decreased freezing time (Figure 6(b), p < 0.001, two-tailed T test), which suggested that APH1a overexpression
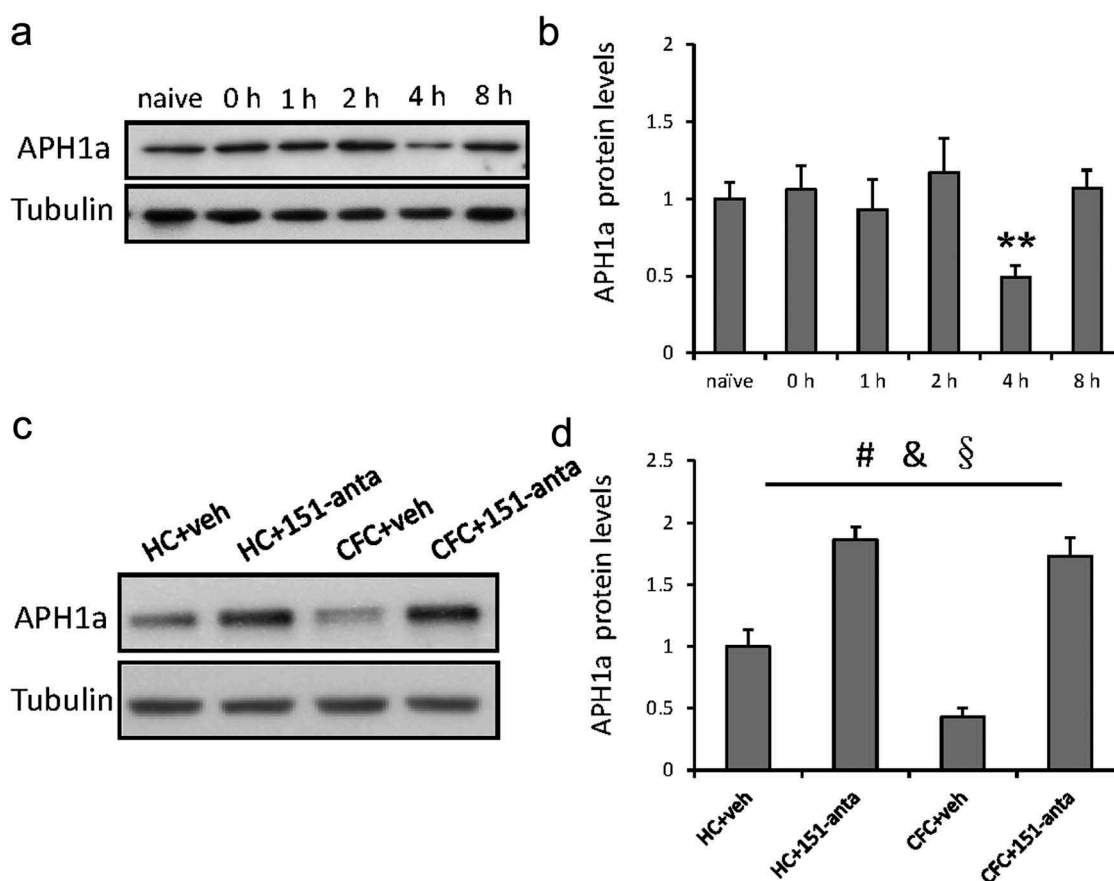
Figure 5. APH1a protein levels after CFC training is induced by miR-151.

(a) Representative immunoblots of APH1a at 0, 1, 2, 4, 8 h after CFC training. B. Representative immunoblots of APH1a protein levels (n = 5–6 per group; **p < 0.01 vs naive group). (c, d) Block miR-151 decreased APH1a protein levels 4 h after CFC training (n = 4 per group; #: significant antagomir effect; &: significant CFC effect; §: significant interaction effect). Representative immunoblots are shown in C, and the relative densitometric analysis is shown in D. All values are presented as the mean ± SEM.

impaired the formation of hippocampus-dependent long-term contextual fear memory. Meanwhile, mice injected with the si-APH1a lentivirus showed increased freezing time in response to a low current intensity (Figure 6(d), p = 0.024, two-tailed T test), which suggested that knockdown of APH1a could enhance the long-term formation of contextual fear memory.

Taken together, these results suggested that APH1a could participate in adult hippocampal contextual fear memory, which is consistent with the functions of miR-151-5p we have found above.

The effect of miR-151 on the long-term contextual fear memory formation depends on APH1a

Our above data revealed that APH1a was involved in the consolidation of contextual fear memory. We then asked whether miR-151 participation in consolidation was dependent on APH1a. Our results showed that miR-151 overexpression enhanced the formation of contextual fear memory (Figure 7(b), miR-151-OE, $F_{(1,39)}$ = 6.004, p = 0.019, two-way ANOVA). Moreover, mice in the APH1a-OE group exhibited less freezing time than mice in the GFP group (Figure 7(b), APH1a-OE, $F_{(1,39)}$ = 82.737, p < 0.001, two-way ANOVA), which suggested that gain APH1a function suppressed the consolidation of contextual fear memory.

However, mice in the miR-151-OE+APH1a-OE group showed significantly decreased freezing time compared with mice in the GFP group (Figure 7(b)), miR-151-OE ×APH1a-OE interaction, $F_{(1,39)}$ = 12.954, p = 0.001, two-way ANOVA), which suggested that gain functions of APH1a could block the miR-151-OE induced contextual fear memory consolidation enhancement. These results indicated that the effect of miR-151 on the contextual fear memory consolidation in the hippocampus depends on APH1a.

Discussion

In this study, we observed that miR-151 was responsible for the formation of contextual fear memory. Using a luciferase reporter assay, we found APH1a was the target of miR-151. Finally, we indicated that up-regulated miR-151 could reduce its target APH1a protein levels and thus promote the formation of contextual fear memory.

Our results provide several new insights into the mechanisms of miRNAs in hippocampus-dependent memory. First, we found that miR-151 was involved in hippocampal contextual fear memory formation in adult mice. miR-151 was revealed to be co-expressed with focal adhesion kinase (FAK) and its involvement in both cancer and cardiac hypertrophy have been investigated [24,28–31]. miR-151 also
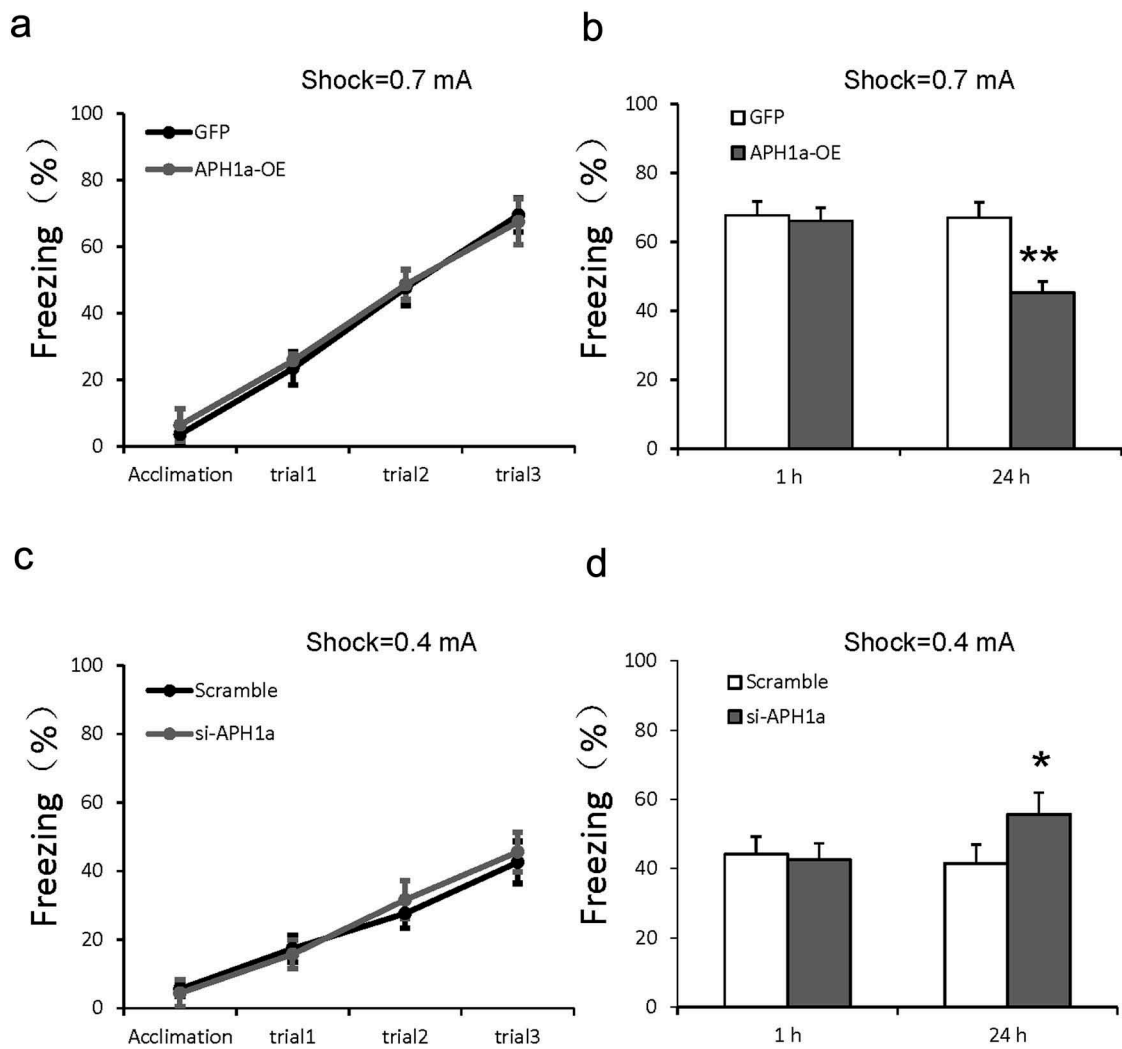
Figure 6. APH1a in the hippocampus is involved in fear memory formation.

(a, b) Elevated APH1a impaired CFC memory formation. (A). The freezing response in training. (b) The freezing responses 1 h and 24 h after training (n = 9–11 per group; **p < 0.01 vs 24 h Scr+veh group). (c, d) Knockdown of APH1a enhanced CFC memory formation following a weak shock. (c) The freezing response in training. (d) The freezing responses 1 h and 24 h after training (n = 9–10 per group; **p < 0.01 vs Scr+veh group). All values are presented as the mean ± SEM.

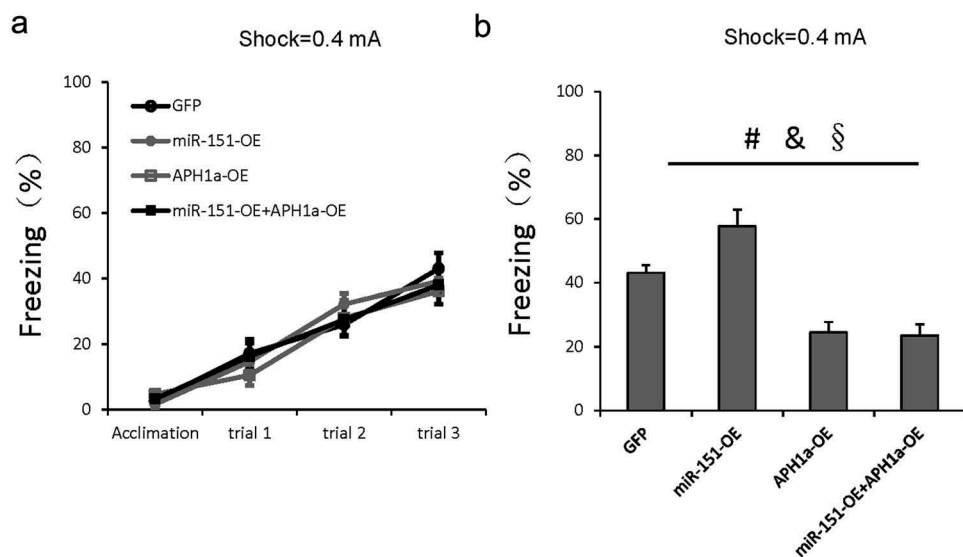**Figure 7.** The effect of miR-151 on the formation of contextual fear memory depends on APH1a.

(a, b) Increased APH1a impaired CFC memory formation enhanced by miR-151-overexpression. (a). The freezing response in training. (b). The freezing response 24 h after training (n = 9–11 per group; #: significant miR-151-OE effect; &: significant APH1a-OE effect; §: significant interaction effect). All values are presented as the mean ± SEM.

increases the migration and invasion of hepatocellular carcinoma and prostate cancer cells [32,33]. However, the roles of miR-151 in the central nervous system are still largely unknown. Our data revealed that the expression of miR-151 was increased after CFC training and knockdown of miR-151 could impair long-term memory formation in response to CFC. In contrast, overexpression of miR-151 enhanced the memory formation when using a weak current stimulus. These results suggest that miR-151 plays an important role in long-term memory formation after CFC. Although previous studies have shown that some miRNAs are involved in learning and memory, our work is the first to show that miR-151 could participate in hippocampal memory.

Second, we found important roles for APH1a in contextual fear memory. APH1a, which forms a stable subcomplex with nicastrin and contributes to the stabilization and trafficking of the γ-secretase complex, was identified as a key factor in γ-secretase activity [34,35]. Two APH1 homologues, APH1a and APH1b, have been identified in humans APH1a [36]. Knockdown of APH1a by small interfering RNA alters the formation of multimeric complexes and significantly reduces the production of Aβ [35,37]. As APH1a is the principal mammalian APH1 isoform within γ-secretase complexes, the overexpression of APH1a can increase γ-secretase activity and cellular Aβ content [38–41]. Previous studies have shown that APH1a is responsible for the cleavage of APP that generates Aβ, one of the primary components of amyloid plaques in AD [42], however, the functions of APH1a in learning and memory remain unknown. Our work provides evidence that increasing APH1a expression in the DG impairs CFC long-term memory formation. Further, decreasing APH1a in the DG enhanced the hippocampal long-term contextual fear memory formation. These results indicate that APH1a in the DG negatively regulates hippocampal contextual fear memory. Our work is the first to identify an important role for APH1a in hippocampus-dependent memory.

Finally, we showed miR-151 participates in hippocampal contextual fear memory by regulating its target APH1a. We used a luciferase reporter assay to identify APH1a as a potential target of miR-151. Our results indicated that inhibiting miR-151 using antagomir could reverse the decrease of APH1a levels after CFC training, which suggested that miR-151 could regulate APH1a levels after CFC training. Our behavioural data showed that upregulating APH1a could impair the formation of contextual fear memory. Moreover, overexpression of miR-151 could not rescue the APH1a upregulation-induced memory deficits. These results indicated that miR-151 participation in hippocampal contextual fear memory formation depends on its target APH1a. Our work is the first to verify that miR-151 participates in hippocampal contextual fear memory in vivo by regulation of its target APH1a.

In conclusion, to the best of our knowledge, we determined for the first time that miR-151 participates in hippocampal contextual fear memory formation. We provided evidence that miR-151 was involved in hippocampal long-term CFC memory formation by decreasing the protein levels of its target, APH1a, in adult mice. Our study will promote better understanding of the functions of miRNAs in learning and memory. Considering that miRNAs are important to many brain disorders, miR-151 is a potentially important therapeutic target that merits further study.

Materials and methods.

Animals

Adult C57BL/6J mice (2–3 months old) were housed in standard cages in a temperature controlled (22 ± 2 °C) room under diurnal conditions (12 h light/dark cycle) with food and water available *ad libitum* unless noted otherwise. All animal procedures were in accordance with the guidelines of the National Institutes of Health Guide for the Care and Use of Laboratory Animals and were approved by the Institutional Animal Care and Use Committee of Shandong University.

Tissue preparation and western blot

Brains were quickly removed after decapitation at the desired time points and coronal sections (1mm thick) were obtained using a mouse brain slicer (Braintree Scientific). Hippocampus regions were obtained freehand at 0°C followed by homogenization using a Bullet Blender Homogenizer (Nextadvance). Rodent tissue homogenates were prepared in Tris-HCl buffer, pH 7.5, containing 1% NP-40, 150 mM NaCl, 1 mM EDTA, and 1 μg/ml leupeptin, 3.8 μg/ml aprotinin, 1 mM PMSF, 1 μg/ml pepstatin, 1 mM Na_3VO_4 and 2 mM NaF. Extracts were clarified by centrifugation at 4°C (14,000 g for 20 minutes). Supernatants were collected and eluted with SDS sample buffer, and the proteins were resolved by SDS-PAGE. Goat anti-APH 1a antibody (Abcam, 1:1000) and the mice anti-α-Tubulin (Sigma, 1:10,000) were respectively used as primary antibodies. Goat anti-mouse or anti-rabbit secondary antibodies (Calbiochem, 1:1000) were used to react with the corresponding primary antibodies. Immunoreactive bands were visualized by enhanced chemiluminescence (ECL, Pierce). Densitometry analysis on the bands was calculated by Quantity One (version 4.6.2, Bio-Rad).

Surgery and Microinjection

Mice were anaesthetized with 5% chloral hydrate (8 ml/kg, i.p.) and placed in the stereotaxic apparatus (8001, RWD Life Science) before the surgery. The coordinates (in reference to bregma) were as follows: lateral (L), ± 1.0 mm; anteroposterior (AP), – 1.70 mm; dorsoventral (V), and – 2.3 mm. The 1×10 [9] unit titer lentivirus with green-fluorescent protein sequence was injected into bilateral DG by microinjection (KDS200, KD Scientific). Infusions were performed at a volume of 1 μl for 2 min and the infusion cannula was left for diffusion for an additional 3 min. The APH1a shRNA sequence used for siAPH1a lentivirus was as follows: APH1a shRNA antisense, 5′ TGGCAACCTGCACTGTCCA3′. The FUGW lentivirus vectors were used to package the target overexpression lentivirus. The miR-151 antagomirs were purchased from RiboBio.Co. and overexpression lentivirus was purchased from GeneCopoeia™.

Luciferase assay

The pmirGLO Dual-Luciferase miRNA Target Expression Vector was purchased from Promega (Cat. # E1330). The primer sequences used were: APH1a forward primer,

5′GGGTTTAAACTAGCGGCCGCCTACCTGGACTGATCG-CCCGACAGA3′, reverse primer, 5′ TGCTCTAGATGACTGGCTGCACCCAGGCTGC3′, mutated APH1a forward primer, 5′ ATCCTCCGTGCAACGTCTGATGTG3′ and mutated APH1a reverse primer, 5′ CACATCAGACGTTGCACGGAGGAT3′. HEK293 cells were cotransfected with the group of Figure 4.

Behaviour

Contextual fear conditioning
On the first day, mice were placed into a standard fear-conditioning chamber (Panlab) for training. Mice were exposed to the conditioning context for 2 min after which three 1 s, 0.4 or 0.7 mA foot shocks were given with an intertrial interval of 59 s. After the last shock, mice were left in the chamber for 59 s before being moved back to their home cages. 1 h and 24 h after training, mice were transferred back to the previous conditioning chamber where training occurred and freezing responses were recorded for 5 min without foot shock.

Cued fear conditioning
Mice were pre-exposed to conditioning chambers (Context A) for 3 consecutive days before training. On the day of training, mice were put in Context A and given 3 CS-US pairings (CS: 30 s, 6 kHz, 75 db tone; US: 1 s, 0.7 mA shock). After the last shock, mice were left in the chamber for 59 s before being moved back to their home cages. 1 h and 24 h after training, mice were transferred back to the previous conditioning chamber where training occurred and freezing responses were recorded for 5 min without foot shock.

Morris water maze
The Morris water maze apparatus included a circular water tank (120 cm diameter, 40 cm height) filled with water (22°C) to a depth of 25 cm, and water was made opaque by the addition of nontoxic white powder paint. A circular escape platform (6 cm in diameter) was placed 1 cm below the water surface. During the learning period, the platform was always placed in the centre of the same quadrant (target quadrant). Each trial consisted of a maximum of 60 s starting from one of the four quadrants with the mice facing the wall. If one mouse could not reach the platform in 60 s, it was guided to the platform. After reaching the platform, mice were allowed to stay there for 30 s, and then quickly dried with a towel and put under a heating lamp set at exactly 37°C to avoid hypothermia. The mice received four trials per day in the water maze on each of the four training days. In the learning process, the escape latencies for a single day were averaged to produce a daily mean. At day 5, the platform was removed, and mice swam for 60 s. The number of platform crossings and the time spent in the four quadrants for each mouse was recorded with a video tracking system (Smart)

Open field test
The open field test consisted of a 40 cm × 40 cm area divided into central (20 cm × 20 cm) and 35 cm high walls. During the test, mice were placed in the centre of the field and behaviour was recorded for 10 min. The video tracking system (Smart) was used to score the distance mice moved and time spent in the field. The total distance travelled in the arena over 10 min was recorded as the index of locomotor activity. Time spent in centre of the open field was used as a measure of anxiety-like behaviour.

Elevated plus maze
The elevated plus maze apparatus was constructed of black stainless steel with four arms (30 cm length × 5 cm width): two open arms with a small raised lip (0.5 cm) and two closed arms with high, black walls (30 cm high). All four arms were connected by a central platform (5 cm × 5 cm). The maze was elevated to 50 cm above the ground. The mouse was placed at the centre of the platform with its head facing an open arm to initiate the 5 min test session. The video tracking system (Smart) was used to measure the number of entries into the open and closed arms and the time spent in the open arms.

RT-PCR
Total RNA was isolated using TRIzol-A+ RNA isolation reagent (Tiangen) following the manufacturer's protocol. A 0.5 μg aliquot of each sample was treated with DNase to avoid DNA contamination, and then was reverse transcribed using the All-in-One™ miRNA qRT-PCR Detection Kit (Cat. No. AOMD-Q020, GeneCopoeiaTM). The reaction was incubated for 60 min at 37°C followed by 5 min at 98°C. Quantitative real time RT-PCR was performed in a Cycler (Bio-Rad) using SYBR-Green (Roche). The primer sequences used were as follows: miR-151 primer, 5′TGATCTGACACTCGAGGAGCT3′ and U6 primer 5′CTCGCTTCGGCAGCACATATACT3′. Each sample was assayed in duplicate and the levels of miRNA were normalized for each well to the levels of U6 using the $2^{-\Delta\Delta CT}$.

Immunochemistry
Mice were anaesthetized with 5% chloral hydrate anaesthesia (8 ml/kg, i.p.) and perfused with 0.9% NaCl solution, followed by 4% paraformaldehyde (PFA), pH 7.6. Brains were post-fixed in 4% PFA overnight followed by equilibration at 4°C in 30% sucrose for another 24 h before sectioning. Brains were sliced into 40 μm coronal section series on a Microm cryostat (HM 550) at − 20°C. The immunohistological staining solution contained 0.3% Triton X-100, 0.1% BSA, 10% normal goat serum, and anti-GFP mice primary antibody (Sigma, 1:200). After a series of 0.1 M phosphate buffer washes, sections were stained using the same blocking solution as above and Alexa Fluor 488 goat anti-mouse secondary antibody (Invitrogen, 1:1000), 594 Fluorescent Conjugates of streptavidin antibody (Invitrogen, 1:1000).

Statistics
CFC training data were analysed by repeated measures two-way ANOVA. Other group differences were analysed using a two-tailed t test or one-way ANOVA, which was followed by LSD post hoc analysis to compare means from several groups simultaneously. Significance was set at $p < 0.05$. Results are expressed as the mean ±SEM. Data analyses were performed using SPSS statistical program, version 13.0.

Acknowledgments

Author Contributions

X.-F.X. designed research; X.-F.X., Y-C.W. and L.Z. performed research; X.-F.X. analyzed data; X.-F.X. and X.-L.W. wrote the paper.

Disclosure statement

No potential conflict of interest was reported by the authors.

ORCID

Xu-Feng Xu http://orcid.org/0000-0003-3235-907X
Liang Zong http://orcid.org/0000-0003-3751-4198

References

[1] Dudai Y. The neurobiology of consolidations, or, how stable is the engram? Annu Rev Psychol. 2004;55:51–86.

[2] Maguschak KA, Ressler KJ. A role for WNT/beta-catenin signaling in the neural mechanisms of behavior. J Neuroimmune Pharmacol. 2012;7:763–773.

[3] Maren S. The amygdala, synaptic plasticity, and fear memory. Ann N Y Acad Sci. 2003;985:106–113.

[4] Silva AJ, Giese KP. Plastic genes are in! Curr Opin Neurobiol. 1994;4:413–420.

[5] Hendershot TJ, Liu H, Clouthier DE, et al. Conditional deletion of Hand2 reveals critical functions in neurogenesis and cell type-specific gene expression for development of neural crest-derived noradrenergic sympathetic ganglion neurons. Dev Biol. 2008;319:179–191.

[6] Zovkic IB, Guzman-Karlsson MC, Sweatt JD. Epigenetic regulation of memory formation and maintenance. Learn Mem. 2013;20:61–74.

[7] Abe M, Bonini NM. MicroRNAs and neurodegeneration: role and impact. Trends Cell Biol. 2013;23:30–36.

[8] Zovoilis A, Agbemenyah HY, Agis-Balboa RC, et al. microRNA-34c is a novel target to treat dementias. Embo J. 2011;30:4299–4308.

[9] Kos A, Olde Loohuis N, Meinhardt J, et al. MicroRNA-181 promotes synaptogenesis and attenuates axonal outgrowth in cortical neurons. Cell Mol Life Sci. 2016.

[10] Siegert S, Seo J, Kwon EJ, et al. The schizophrenia risk gene product miR-137 alters presynaptic plasticity. Nat Neurosci. 2015;18:1008–1016.

[11] Schratt G. Fine-tuning neural gene expression with microRNAs. Curr Opin Neurobiol. 2009;19:213–219.

[12] Dias BG, Goodman JV, Ahluwalia R, et al. Amygdala-dependent fear memory consolidation via miR-34a and Notch signaling. Neuron. 2014;83:906–918.

[13] Lin Q, Wei W, Coelho CM, et al. The brain-specific microRNA miR-128b regulates the formation of fear-extinction memory. Nat Neurosci. 2011;14:1115–1117.

[14] Spadaro PA, Bredy TW. Emerging role of non-coding RNA in neural plasticity, cognitive function, and neuropsychiatric disorders. Front Genet. 2012;3:132.

[15] Wang W, Kwon EJ, Tsai LH. MicroRNAs in learning, memory, and neurological diseases. Learn Mem. 2012;19:359–368.

[16] Xu XF, Jing X, Ma HX, et al. miR-181a participates in contextual fear memory formation via activating mtor signaling pathway. Cereb Cortex. 2018;28:3309–3321.

[17] Cogswell JP, Ward J, Taylor IA, et al. Identification of miRNA changes in Alzheimer's disease brain and CSF yields putative biomarkers and insights into disease pathways. J Alzheimers Dis. 2008;14:27–41.

[18] Alexandrov PN, Dua P, Hill JM, et al. microRNA (miRNA) speciation in Alzheimer's disease (AD) cerebrospinal fluid (CSF) and extracellular fluid (ECF). Int J Biochem Mol Biol. 2012;3:365–373.

[19] Absalon S, Kochanek DM, Raghavan V, et al. MiR-26b, upregulated in Alzheimer's disease, activates cell cycle entry, tau-phosphorylation, and apoptosis in postmitotic neurons. J Neurosci. 2013;33:14645–14659.

[20] Dorval V, Nelson PT, Hebert SS. Circulating microRNAs in Alzheimer's disease: the search for novel biomarkers. Front Mol Neurosci. 2013;6:24.

[21] Lau P, Bossers K, Janky R, et al. Alteration of the microRNA network during the progression of Alzheimer's disease. EMBO Mol Med. 2013;5:1613–1634.

[22] Singh A, Sen D. MicroRNAs in Parkinson's disease. Exp Brain Res. 2017;235:2359–2374.

[23] Wei H, Li Z, Wang X, et al. microRNA-151-3p regulates slow muscle gene expression by targeting ATP2a2 in skeletal muscle cells. J Cell Physiol. 2015;230:1003–1012.

[24] Livak KJ, Schmittgen TD. Analysis of relative gene expression data using real-time quantitative PCR and the 2(-Delta Delta C(T)) Method. Methods. 2001;25:402–408.

[25] Monzon FA, Alvarez K, Peterson L, et al. Chromosome 14q loss defines a molecular subtype of clear-cell renal cell carcinoma associated with poor prognosis. Mod Pathol. 2011;24:1470–1479.

[26] Taylor BS, Schultz N, Hieronymus H, et al. Integrative genomic profiling of human prostate cancer. Cancer Cell. 2010;18:11–22.

[27] Luedde T. MicroRNA-151 and its hosting gene FAK (focal adhesion kinase) regulate tumor cell migration and spreading of hepatocellular carcinoma. Hepatology. 2010;52:1164–1166.

[28] Lips EH, van Eijk R, de Graaf EJ, et al. Integrating chromosomal aberrations and gene expression profiles to dissect rectal tumorigenesis. BMC Cancer. 2008;8:314.

[29] Sayed D, Hong C, Chen IY, et al. MicroRNAs play an essential role in the development of cardiac hypertrophy. Circ Res. 2007;100:416–424.

[30] Wong MP, Fung LF, Wang E, et al. Chromosomal aberrations of primary lung adenocarcinomas in nonsmokers. Cancer. 2003;97:1263–1270.

[31] Climent J, Dimitrow P, Fridlyand J, et al. Deletion of chromosome 11q predicts response to anthracycline-based chemotherapy in early breast cancer. Cancer Res. 2007;67:818–826.

[32] Ding J, Huang S, Wu S, et al. Gain of miR-151 on chromosome 8q24.3 facilitates tumour cell migration and spreading through downregulating RhoGDIA. Nat Cell Biol. 2010;12:390–399.

[33] Chiyomaru T, Yamamura S, Zaman MS, et al. Genistein suppresses prostate cancer growth through inhibition of oncogenic microRNA-151. PLoS One. 2012;7:e43812.

[34] Yonemura Y, Futai E, Yagishita S, et al. Specific combinations of presenilins and Aph1s affect the substrate specificity and activity of gamma-secretase. Biochem Biophys Res Commun. 2016;478:1751–1757.

[35] Meckler X, Roseman J, Das P, et al. Reduced Alzheimer's disease ss-amyloid deposition in transgenic mice expressing S-palmitoylation-deficient APH1aL and nicastrin. J Neurosci. 2010;30:16160–16169.

[36] Saito S, Araki W. Expression profiles of two human APH-1 genes and their roles in formation of presenilin complexes. Biochem Biophys Res Commun. 2005;327:18–22.

[37] Lessard CB, Cottrell BA, Maruyama H, et al. Gamma-secretase modulators and aph1 isoforms modulate gamma-secretase cleavage but not position of epsilon-cleavage of the amyloid precursor protein (APP). PLoS One. 2015;10:e0144758.

[38] Mamada N, Tanokashira D, Ishii K, et al. Mitochondria are devoid of amyloid beta-protein (Abeta)-producing secretases: evidence for unlikely occurrence within mitochondria of Abeta generation from amyloid precursor protein. Biochem Biophys Res Commun. 2017;486:321–328.

[39] Wang R, Zhang YW, Zhang X, et al. Transcriptional regulation of APH-1A and increased gamma-secretase cleavage of APP and Notch by HIF-1 and hypoxia. FASEB J. 2006;20:1275–1277.

[40] Marchesi VT. An alternative interpretation of the amyloid Abeta hypothesis with regard to the pathogenesis of Alzheimer's disease. Proc Natl Acad Sci U S A. 2005;102:9093–9098.

[41] Ma G, Li T, Price DL, et al. APH-1a is the principal mammalian APH-1 isoform present in gamma-secretase complexes during embryonic development. J Neurosci. 2005;25:192–198.

[42] De Strooper B. Aph-1, Pen-2, and Nicastrin with presenilin generate an active gamma-secretase complex. Neuron. 2003;38:9–12.